

Entangling power of quantized chaotic systems

Arul Lakshminarayan

Physical Research Laboratory, Navrangpura, Ahmedabad 380 009, India

(Received 4 December 2000; published 20 August 2001)

We study the quantum entanglement caused by unitary operators that have classical limits that can range from the near integrable to the completely chaotic. Entanglement in the eigenstates and time-evolving arbitrary states is studied through the von Neumann entropy of the reduced density matrices. We demonstrate that classical chaos can lead to substantially enhanced entanglement. Conversely, entanglement provides a useful characterization of quantum states in higher-dimensional chaotic or complex systems. Information about eigenfunction localization is stored in a graded manner in the Schmidt vectors, and the principal Schmidt vectors can be scarred by the projections of classical periodic orbits onto subspaces. The eigenvalues of the reduced density matrices is sensitive to the degree of wave-function localization, and is roughly exponentially arranged. We also point out the analogy with decoherence, as reduced density matrices corresponding to subsystems of fully chaotic systems, are diagonally dominant.

DOI: 10.1103/PhysRevE.64.036207

PACS number(s): 05.45.Mt, 03.67.-a, 03.65.Yz

I. INTRODUCTION

Entanglement has been studied since the early days of quantum mechanics and provides the essential ingredient of Einstein-Podolsky-Rosen phenomena [1]. It results when the state of a system, which is composed of at least two subsystems, cannot be written as a product of states that reside entirely in the subsystems. This leads to the well-known unique quantum correlations that exist even in spatially well-separated pairs of particles. More recently, entanglement has been discussed extensively in the context of quantum information theory. It has been recognized as a quantum resource for quantum superdense coding and quantum teleportation, while helping to make quantum computations qualitatively superior to classical ones [2].

Usually the entangled subsystems are distinct identical particles and the entanglement is created by symmetrization, such as in the spin singlet state of a fermionic pair. However, entanglement may of course be created during time evolution due to conventional interactions of a potential nature. In this case, the “subsystems” may also be the many degrees of freedom of the same particle. This is more general than the special case wherein the interaction preserves the permutation symmetry between the say d (formal) degrees of freedom, and may therefore be interpreted as representing d identical particles in one dimension.

Presented with the inexpensive resource of unentangled states, unitary operations may be devised to create potentially useful entangled states. Thus an understanding of the range of entanglement produced by the wide range of unitary operations is of interest. If these unitary operators are generated from Hamiltonians, then a natural question that arises is the connection between the dynamics generated by the Hamiltonian and the entanglement produced. In particular it has been recognized for some time now that the two extreme cases of classical dynamics, namely, the completely integrable and the completely chaotic [3], leave remarkably different traces on quantization [4]. In this paper we inquire into the possible effects of quantum chaos on quantum entanglement.

Entanglement in eigenstates of some Hamiltonians have begun to be studied. Largely, Hamiltonians from condensed-matter physics have drawn attention as some form of spin chains are possible realizations of quantum registers. For instance, the ground state of an antiferromagnetic model has been recently studied [5] in this context while entanglement in the Ising one-dimensional (1D) model has also been investigated [6]. Previously the connection between entanglement and quantum dynamical manifestation of chaos has been studied with the example of the N -atom Jaynes-Cummings model [7]. It was found that decoherence rates are considerably enhanced if the initial wave packet was placed in a “chaotic” region; that is its phase-space representation, was dominated by a classically chaotic region. In another work of a similar kind [8], the authors have studied the linear entropy production in coupled kicked tops and related the rates to classical Lyapunov exponents. Thus this paper, which concentrates on stationary states and quantum scarring, may contribute to furthering our understanding of entanglement produced by qualitatively different dynamics. A related issue is that of decoherence [9] and our treatment is equivalent to treating the environment as a subsystem of a quantum chaotic system, and may be seen in the context of a body of work that has arisen wherein dephasing is studied with the environmental degrees of freedom being either random matrices [10] or low-dimensional chaotic systems [11].

Certain finite unitary matrices have been studied extensively in the quantum chaos literature and represent a rich source of operators with a wide range of well-understood dynamical behaviors in the classical limit. They may, for instance, arise naturally while quantizing symplectic maps on the torus [12–14]. However, most of the studies have been limited to the two torus, with essentially one degree of freedom, while entanglement studies necessarily deal with the entanglement between two subsystems. Thus, while two degree of freedom Hamiltonian flows lead to one degree of freedom maps, we need to consider at least a four-dimensional symplectic map to study entanglement directly. Another possibility is to treat a finite dimensional Hilbert space (of appropriate dimensionality) as isomorphic to a

product space of say qubits, as done for instance for the quantum baker's map [15], and consider the entanglement among the qubits.

We use a coupled quantum standard map as the model system. The standard map is well-understood classically, there is a smooth transition from the regular to the chaotic, and it has been the object of several quantum investigations as well (reviewed in Ref. [14]), including an experimental realization [16]. The coupled map has been studied classically, principally, to understand Arnol'd diffusion [17]. Thus our results below also represent new results in the largely sparse literature on higher-dimensional ($d > 1$ for maps, $d > 2$ for flows) quantum chaotic systems. In particular, we explore the usefulness of entanglement as a measure of quantum chaos for such systems. Our results, largely exploratory and numerical in nature, quantify what is intuitively (and certainly linguistically) evident; the connection between entanglement and chaos. The larger the chaos, the more the entanglement that is induced by the dynamics, as opposed to entanglement due to symmetries. However we also find, interestingly, that the reduced density matrices store information about localization of certain states in a systematic manner. By localization, we refer to localization in the combined full Hilbert space. To be specific we refer to "phase-space" localization or the phenomenon of quantum scars [18]. The states that are most vividly scarred are also those that are nearly separable, in terms of single-particle states, and therefore we should expect that these have low entanglement. More detailed work is needed to comment on generic scarred states.

Consider a bipartite quantum system whose state space is $\mathcal{H} = \mathcal{H}_1 \otimes \mathcal{H}_2$, where $\dim \mathcal{H}_i = N$ ($i = 1, 2$). The unitary operator acts on vectors in the space \mathcal{H} , where $\dim \mathcal{H} = N^2$. We consider the case where the two subsystems have the same dimensionality. Let $|\psi\rangle \in \mathcal{H}$, and the reduced density matrices be $\rho_1 = \text{Tr}_2(|\psi\rangle\langle\psi|)$ and $\rho_2 = \text{Tr}_1(|\psi\rangle\langle\psi|)$, where the first matrix is obtained by tracing out the second degree of freedom and the second by tracing out the first. The von Neumann entropy S , referred to in the rest of the paper as simply entropy, of the reduced density matrices, measures the entanglement of the pure state $|\psi\rangle$ in an essentially unique manner

$$S = -\text{Tr}_1(\rho_1 \ln(\rho_1)) = -\text{Tr}_2(\rho_2 \ln(\rho_2)). \quad (1)$$

The close analogy between this entropy and thermodynamic entropy has been noted and discussed earlier [19].

The eigenvalues of the reduced density matrices form the (square of the) coefficients of the Schmidt decomposition. This decomposition expresses the state in the full Hilbert space as a linear combination of N product states [1] instead of N^2 that is evident. If we were to write the eigenvector, for instance, in the position basis and in the Schmidt decomposed forms, we would have

$$|\psi\rangle = \sum_{n_1, n_2} c_{n_1, n_2} |n_1\rangle |n_2\rangle = \sum_{j=1}^N \sqrt{\lambda_j} |\phi_j\rangle^S |\phi_j'\rangle^S. \quad (2)$$

A simple proof of this is also found in the Appendix of Ref. [20]. Thus there is a basis in each Hilbert space such that each basis vector in \mathcal{H}_1 is uniquely correlated with the one in \mathcal{H}_2 as far as the state $|\psi\rangle$ is concerned. The states $|\phi_j\rangle^S$ and $|\phi_j'\rangle^S$ are the eigenvectors of the reduced density matrices, and form the basis of the Schmidt decomposition. The Schmidt decomposition is not merely a mathematical convenience but is understood to provide a deeper understanding of correlations between subsystems.

In the literature on quantum chaos or localization [14, 21], the Shannon entropy has often been calculated, and for the above state it is given by

$$S_{shan}(|\psi\rangle) = - \sum_{n_1, n_2} |c_{n_1, n_2}|^2 \ln(|c_{n_1, n_2}|^2). \quad (3)$$

This quantity is, of course, basis dependent and vanishes if the basis is chosen to have a direction along $|\psi\rangle$. The von Neumann entropy or entanglement is, to an important extent, immune to arbitrariness by being invariant under *local* unitary transformations, even though such is not the case for the Shannon entropy. Local transformations are those that act only on individual subspaces. Indeed as long as we have identified our subsystems, entanglement provides an invariant measure. We wish to explore if it can also function as a measure of the complexity of the state. The question is not if the "complex" or complex looking states are always entangled, but whether it is generic for eigenstates of a Hamiltonian to have a strong correlation between entanglement and other measures of complexity.

II. FOUR-DIMENSIONAL STANDARD MAP

We now define the four-dimensional (4D) standard map [17]. It is composed of two pendulums that are periodically kicked and are also coupled to each other. The symplectic transformation of the phase-space variables (q_1, q_2, p_1, p_2) , connecting states just before two consecutive kicks, separated by unit time, is the classical map

$$q_1' = q_1 + p_1', \quad (4a)$$

$$p_1' = p_1 + \frac{K_1}{2\pi} \sin(2\pi q_1) + \frac{b}{2\pi} \sin(2\pi(q_1 + q_2)), \quad (4b)$$

$$q_2' = q_2 + p_2', \quad (4c)$$

$$p_2' = p_2 + \frac{K_2}{2\pi} \sin(2\pi q_2) + \frac{b}{2\pi} \sin(2\pi(q_1 + q_2)). \quad (4d)$$

The phase space is restricted to the unit four-torus T^4 , and therefore mod 1 operations are understood in all of Eq. (4). If $b = 0$, the system falls into two uncoupled standard maps. In this limit, much is known of the dynamics [3]; briefly, if $K = 0$ (referring now to either K_1 or K_2), the dynamics is integrable, while at $K \approx 1$, the last KAM rotational tori breaks, heralding large-scale diffusion in the phase space, for $K < 5$, the phase space is that of a typical Hamiltonian system, a mixed phase space with both regular and chaotic re-

gions. When $K \gg 5$, the dynamics are practically completely chaotic with possible appearances of very tiny stable islands through tangent bifurcations. For $b \neq 0$, little is known, due to the dimensionality of the phase space, although this map has been used in studies of Arnol'd diffusion. We suggest, and substantiate below, that in cases such as these, where finite unitary matrices may be constructed as quantization, the quantum maps can be used to actually find transitions to classical chaos. As we noted for the general case earlier, in the case where $K_1 = K_2$, the system possesses permutation symmetry between the two degrees of freedom and may be interpreted as *two* interacting particles in a 1D standard map external potential.

The quantization of the symplectic transformation in Eq. (4) is a finite unitary matrix, whose dimensionality is N^2 , and $N = 1/h$, where h is a scaled Planck constant. The classical limit is the large N limit. The quantization is straightforward as there exists a kicked Hamiltonian generating the classical map. The quantum standard map on the two torus in the position representation is

$$\begin{aligned}
 U(n', n; K_1, \alpha, \beta) &= \frac{1}{N} \exp\left(-iN \frac{K_1}{2\pi} \cos\left(\frac{2\pi}{N}(n + \alpha)\right)\right) \\
 &\times \sum_{m=0}^{N-1} \exp\left(-\frac{\pi i}{N}(m + \beta)^2\right) \\
 &\times \exp\left(\frac{2\pi i}{N}(m + \beta)(n - n')\right). \quad (5)
 \end{aligned}$$

The position kets are labeled by $n = 0, N-1$ and the position eigenvalues are $(n + \alpha)/N$ while the momentum eigenvalues are $(m + \beta)/N$, $m = 0, \dots, N-1$. Here α and β are real numbers in $[0, 1)$ which represent quantum boundary conditions and are convenient devices for breaking phase-space reflection symmetry (the phase α) and time-reversal symmetry (the phase β). The 4D quantum map is but a simple extension:

$$\begin{aligned}
 \langle n'_1 n'_2 | \mathcal{U} | n_1 n_2 \rangle &= U(n'_1, n_1; K_1, \alpha, \beta) U(n'_2, n_2; K_2, \alpha, \beta) \\
 &\times \exp\left\{-iN \frac{b}{2\pi} \cos\left[\frac{2\pi}{N}(n_1 + n_2 + 2\alpha)\right]\right\}. \quad (6)
 \end{aligned}$$

\mathcal{U} is a unitary matrix in \mathcal{H} , and will induce mixing between the two subsystems. We have assumed the quantum phases in both the subsystems to be identical. Throughout this paper we use $\alpha = 0.35$ and $\beta = 0$ as the quantum phases.

III. RESULTS

A. Stationary state properties

If $b \neq 0$, an unentangled initial state, such as $|n_1, n_2\rangle \equiv |n_1\rangle \otimes |n_2\rangle$, would eventually get entangled by the repeated action of the unitary operator \mathcal{U} . The entangling properties depend on the entanglement already inherent in the stationary states or eigenstates $|\psi_i\rangle$, $i = 1, \dots, N^2$, of \mathcal{U} . Thus we

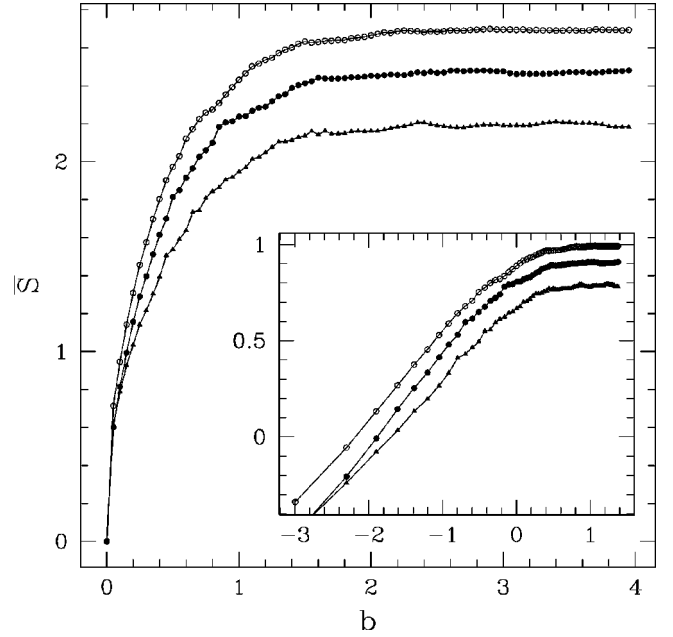


FIG. 1. Average entropy as a function of the coupling b . From top to bottom: the cases correspond to $N = 25, 20$, and 15 , respectively. The inset is a \ln - \ln plot of the same.

first calculate the average entropy of the eigenstates when $K_1 = 0.1, K_2 = 0.15$ as a function of the coupling constant b . At these values of K_i , the uncoupled standard maps are almost wholly regular. We calculate

$$\bar{S} = \frac{-1}{N^2} \sum_{i=1}^{N^2} \text{Tr}_1(\rho_{1i} \ln(\rho_{1i})), \quad \rho_{1i} = \text{Tr}_2(|\psi_i\rangle\langle\psi_i|), \quad (7)$$

where ρ_{1i} is the reduced density matrix after tracing out the second degree of freedom. The quantity \bar{S} is a gross quantity averaged over the entire spectrum, and gives an idea of the average entanglement we can expect on using the operator \mathcal{U} . In Fig. 1 we see the entropy increasing from zero at $b = 0$ and attaining a nearly constant value beyond $b \approx 3$.

The increase in the entropy proceeds along with a gradual increase of chaos in the system, flattening out after considerably uniform chaos has been achieved, a fact that is confirmed by iterating the classical map, Eq. (4). In fact this suggests a compact way of exploring the *classical* transition to chaos, which is otherwise mired in problems of visualizing 4D sections. Thus entanglement is clearly a function of the nature of the underlying classical dynamics. That the entropy increases as an approximate power law before flattening out is shown in the inset. Roughly we get $\bar{S} \approx b^4$. We note here that the Shannon entropy would behave differently, since even when $b = 0$ there is a nonzero Shannon entropy, in general. If there is large scale chaos in the subsystems (as in our model if K_1 and K_2 are greater than five) it will be reflected as a large Shannon entropy; however the entanglement would be zero. For large coupling between the subsystems, both the entropies appear to be well correlated.

Subject to the constraint that $\text{Tr}_1(\rho_{1i}) = 1$, the maximum entropy is $\ln(N)$, and corresponds to the “microcanonical

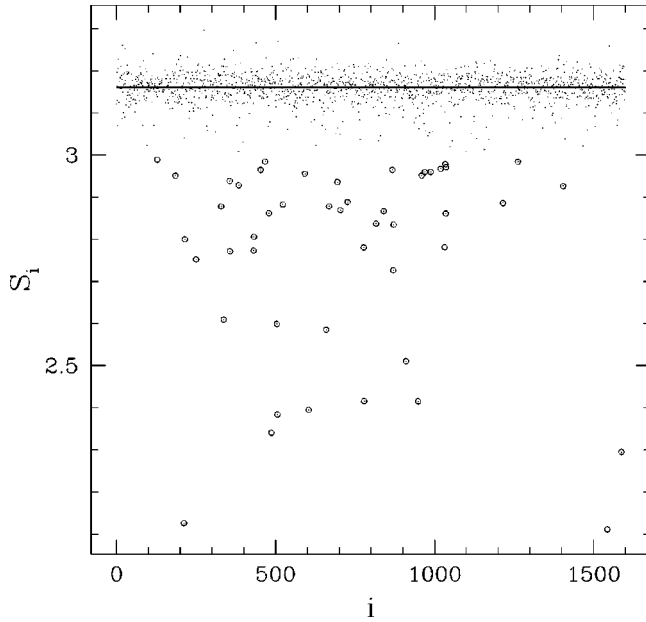


FIG. 2. Entropy of all the 1600 states for the case $K_1=0.1$, $K_2=0.15$, $b=2$, and $N=40$. The straight line is at the value $\ln(0.59N)$, while the states below an entropy of 3 are indicated by circles. The localized state ($i=212$) is the second encircled point.

ensemble” with all the eigenvalues ($\lambda_j, j=1, \dots, N$) of ρ_{1i} being equal to $1/N$. The entanglement entropy induced by the dynamics of quantum chaos falls short of this and in fact the eigenvalues, if arranged in decreasing order, are exponential and reminiscent of the “canonical” ensemble; see the discussion below. From the data of Fig. 1, it appears that at saturation $\bar{S} \approx \ln(0.59N)$. Thus roughly $0.59N$ pairs of correlated states from the two subspaces, make up a typical state. The meaning of this is that of the optimal minimum number of components present in the full state, given the freedom to choose a basis from each subspace. If we are given such a choice in the full Hilbert space, we would have just one component with the basis having one of its directions aligned along the eigenstate, and the von Neumann entropy of the pure state at zero. This may also be compared to an M -dimensional random matrix eigenvector, belonging to the Gaussian orthogonal ensemble (GOE) [22] whose Shannon entropy is approximately $\ln(0.5M)$.

We turn now to a somewhat more detailed study of the entanglement inherent in individual eigenstates. In Fig. 2 is plotted the individual entropies corresponding to all the states of a fairly chaotic system. While most of the states have already achieved the entropy corresponding to the saturation value of $\ln(0.59N)$ (small dots), there are many states that are prominently low in entanglement (those with an entropy less than 3 are marked with a circled dot). The Shannon entropy, not displayed here, of the (small dot) states is to a large accuracy $\ln(0.5N^2)$ (as the dimensionality is $M=N^2$), while there are also minima that largely match those in Fig. 2; therefore these are expected to be localized states. In Fig. 3 is shown two wave functions, one a typical chaotic state and the other a localized state corresponding to the first prominent minima of the entanglement entropy shown in Fig. 2 ($i=212$).

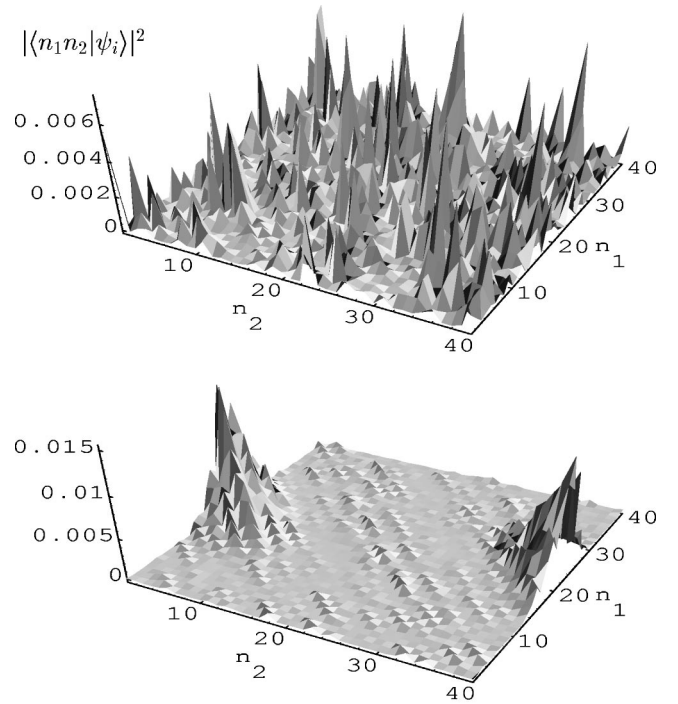


FIG. 3. Eigenfunctions ($|\langle n_1, n_2 | \psi_i \rangle|^2$) of a typical state (top, $i=6$) and a localized state (bottom, $i=212$). Parameter values are the same as that of the previous figure.

Many of the low entropic states are similar to the localized state in Fig. 3, and suggests a “scarring” [18] mechanism. In fact this results from a scarring due to a fixed point of *mixed* stability, and may be called semiscarred if one is to strictly define scarring as due to unstable, hyperbolic orbits [23]. The initial condition ($q_1=0.5, p_1=0, q_2=0, p_2=0$) is a fixed point for all values of the parameters. When $b=2$, the eigenvalues of the Jacobian at this point has a real pair, corresponding to hyperbolic motions and a complex-conjugate pair corresponding to stable motions. This fixed point is poised to completely lose stability just after 2 (at ≈ 2.01). While providing a new example of scarring in higher-dimensional systems due to orbits of mixed stability type, this shows that entanglement is sensitive to eigenfunction localization or scarring. We might expect this to be true for a large class of strongly scarred states.

The structure of the reduced density matrices corresponding to these two states are displayed in Fig. 4 and reveal the connection to decoherence phenomena. The reduced density matrices are typically diagonally dominant in the presence of large-scale chaos. It is interesting that the localized states are more “cleanly” diagonal than the typically delocalized state. There is a rather rapid transition from a nondiagonal to a predominantly diagonal density matrix as the system undergoes a transition to chaos; even mixed phase spaces seem to lead to sufficiently diagonal density matrices. This is shown in Fig. 5 where the average (of the absolute value squared) of the density matrices corresponding to the entire spectrum, is shown. The reduced density matrices of nonstationary states also tend to a diagonal structure very rapidly when the system is chaotic, as will be demonstrated later.

Due to the reduced density matrices being diagonally

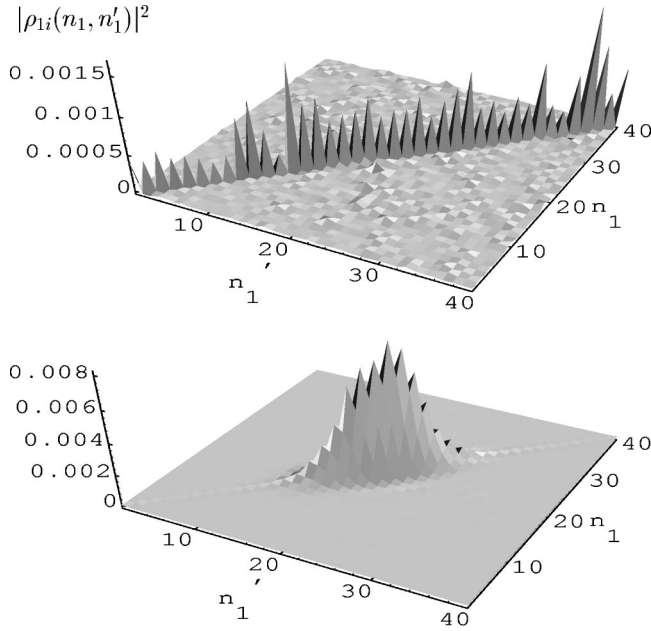


FIG. 4. The reduced density matrices ($|\rho_{1i}|$), obtained by tracing out the second degree of freedom, for the delocalized state (top, $i=6$) and the localized state (bottom, $i=212$) of the previous figure.

dominant, it is not obvious if they themselves have random matrix properties. However the state in the full Hilbert space possesses properties of eigenvectors of random matrices of the GOE (or COE) type. We may then use this to understand the typical diagonal nature of the reduced density matrices. The diagonal term is (dropping the state index i in favor of

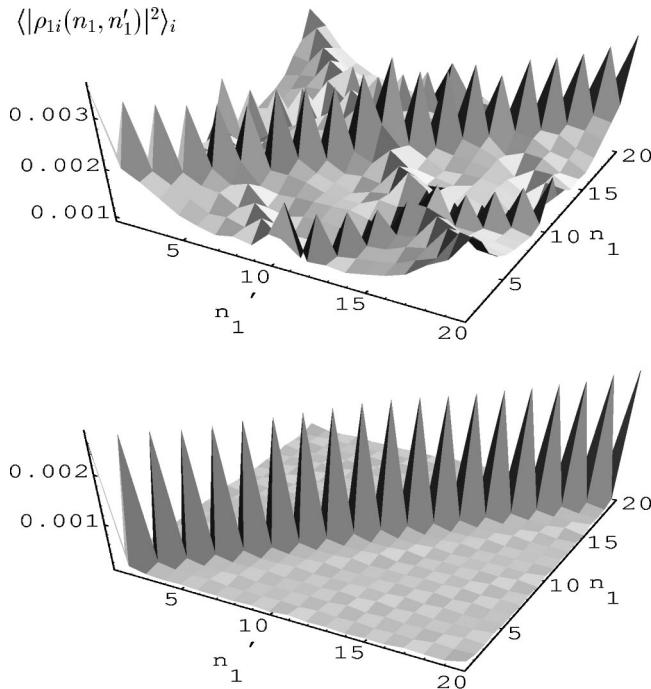


FIG. 5. The spectral average of the square of the elements of the reduced density matrices for the cases of $b=0.05$ (above) and $b=2$ (below). $N=20$, $K_1=0.1$, and $K_2=0.15$ in this figure.

the indices indicating the position in the reduced density matrix):

$$\rho_{1nn} = \sum_k |\langle n k | \psi \rangle|^2. \quad (8)$$

A typical (ensemble averaged) value of $|\langle n k | \psi \rangle|^2$ is $1/N^2$, which one can see easily from the normalization condition. Therefore the typical diagonal element is of order $1/N$. The “strength” of the diagonal elements, as measured in the spectral average, and shown in Fig. 5, will be

$$\langle |\rho_{1nn}|^2 \rangle \sim \frac{1}{N^2}. \quad (9)$$

The off-diagonal element is given by

$$\rho_{1nn'} = \sum_k \langle n k | \psi \rangle \langle \psi | n' k \rangle. \quad (10)$$

The ensemble average of this quantity vanishes. The strength of these elements is

$$\langle |\rho_{1nn'}|^2 \rangle \sim \left\langle \sum_k |\langle n k | \psi \rangle \langle \psi | n' k \rangle|^2 \right\rangle \sim N \frac{1}{(N^2)^2} = \frac{1}{N^3}, \quad (11)$$

where we have used the GOE result [22] that

$$\langle \langle |\langle i | \psi \rangle \langle \psi | i' \rangle|^2 \rangle \rangle = \frac{1}{M(M+2)} \approx \frac{1}{M^2} \quad (i \neq i'), \quad (12)$$

and $M=N^2$ is the dimensionality of the matrix. Thus the average off-diagonal element will be smaller than the diagonal by a factor of \sqrt{N} . This is borne out to a large extent by the numerical results. The reduced density matrices are diagonally dominant and not completely diagonal. The argument used above from assumptions of random matrices and substantiated by numerical calculations, indicate that this diagonal property will be preserved for any local basis and that there is nothing special about the position states.

Is there any advantage in using the reduced density matrix, rather than say the Shannon entropy as a measure of eigenfunction properties, in particular of localization? Clearly the reduced density matrix contains much more by way of information, and the von Neumann entropy derived from it is just one piece of information that gives a global idea of localization. If we have the complementary reduced density matrix obtained by tracing out the first degree of freedom we will have complete information about the wave function, via the Schmidt decomposition. We now study the spectral properties of the reduced density matrices and observe how information about localization is stored in a remarkably graded manner.

The eigenvalues ($\lambda_j; j=1, \dots, N$) of the reduced density matrix, assumed to be arranged in increasing order, also naturally contain information about localization. As we noted earlier these eigenvalues fall off exponentially as seen in Fig. 6. The localized state seems to have at least two exponential

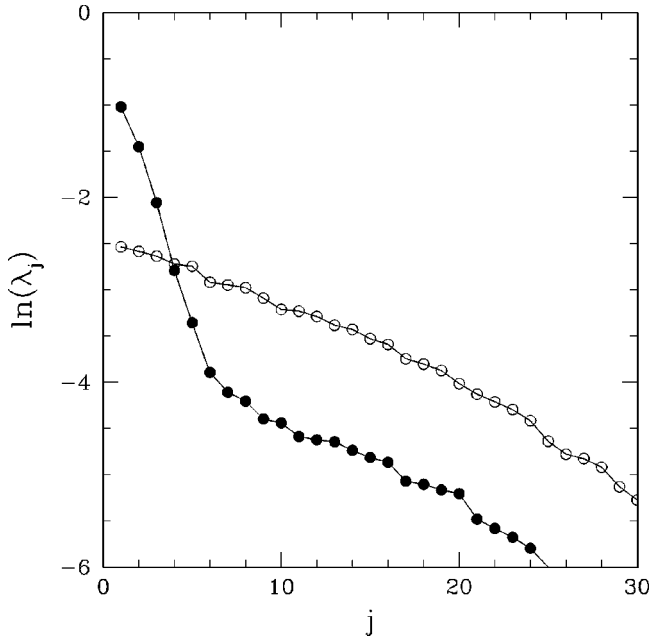


FIG. 6. Principal eigenvalues of the two reduced density matrices in Fig. 4 are shown with the open circles and the closed circles corresponding to the delocalized and localized states, respectively. Note that the scale is \ln linear.

scales while the generic delocalized state has only one. For the latter class of states, we find numerically that

$$\lambda_j \sim \exp\left(-\frac{\gamma j}{N}\right), \quad (13)$$

where γ is an N independent constant. While this is valid for a few of the most significant eigenvalues, there is a clear

deviation of this for smaller eigenvalues and the exponential law seems modulated by a polynomial one that we will not investigate in more detail.

The role of the “temperature” is played by the Hilbert space dimensionality N . This may be compared to the “temperature of the eigenvalue gas,” which measures the equilibrium (fully chaotic) distribution of the level velocities, which is also proportional to N , but the proportionality constant (the “Boltzmann constant”) may be a measure of system specific classical correlations [24]. The localized state seems to be cleanly split into two parts, one with a localization dominant part, and the other that behaves like a generic extended state. The degree to which there are two distinguishable scales depends on the particular localized state. Thus the information about the state’s localization is present in the first few Schmidt states of the reduced density matrix.

We now study the corresponding eigenvectors of the reduced density matrices. These are the Schmidt states $|\phi_j\rangle^S$ in the expansion of Eq. (2) for eigenstates. Since these are in N -dimensional subspaces spanned by either degree of freedom, they correspond classically to “projections in the (q_i, p_i) space.” Here $i=1,2$ while tracing out the second or the first degree of freedom, respectively. We see them in two ways: one is the usual position basis, the other is a phase-space representation, such as a Husimi distribution. The latter will reveal phase-space scarring effects, provided of course that we know enough about the classical dynamics.

The position basis representation of some of the principal eigenvectors or the Schmidt vectors of the reduced density matrices of two states, is shown in Fig. 7. One of these states is a typical nonlocalized state while the other is the localized state discussed above. While the Schmidt vectors of the non-localized state are essentially unremarkable and appear to be random, those that belong to the localized state are them-

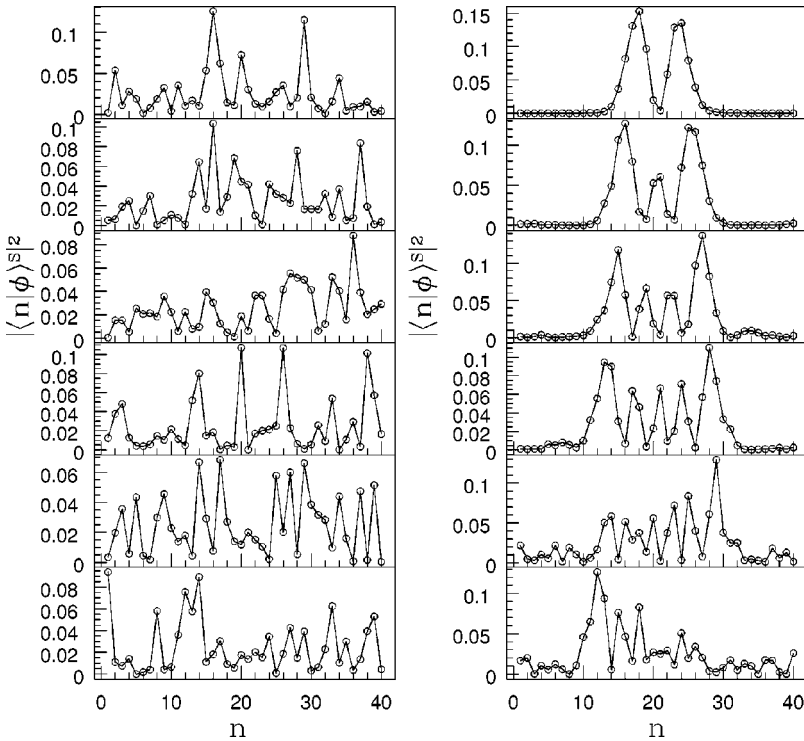


FIG. 7. The six principal Schmidt vectors for a typical chaotic state (left) and for the localized state ($i=212$) (right).

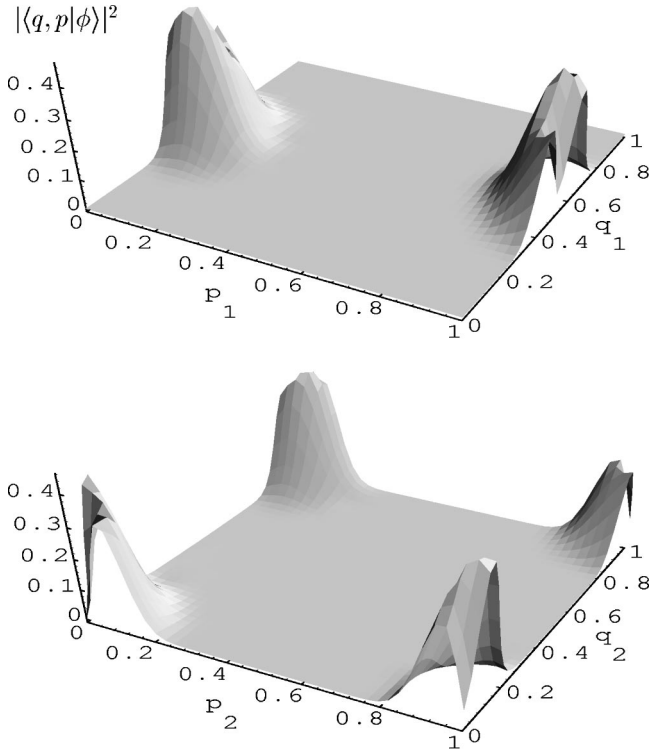


FIG. 8. The Husimi representation $W(q,p)$ of the principal Schmidt vectors of the localized state ($i=212$). The top corresponds to tracing out the second degree of freedom and the bottom the first.

selves localized and appear arranged in the manner typical of eigenstates with increasing node numbers. Beyond the six states shown here, Schmidt vectors of the localized state also look random and indistinguishable from the delocalized state, as is already evidenced in the sixth state. This agrees with the fact that the eigenvalues of the Schmidt vectors also seem to share common trends beyond this point. Thus information about state localization is stored in the Schmidt vectors in a graded manner.

The Husimi of the Schmidt vectors will reveal more about the classical structures that influence the localization. We have asserted previously that the localized state we have been analyzing is influenced by the fixed point $(0.5,0,0,0)$. While this is plausible from the state vector in the position basis already displayed, it is confirmed by the Husimi of the Schmidt vectors. Thus we plot

$$W(q,p) = |\langle q,p|\phi\rangle|^2$$

in Fig. 8, where $|q,p\rangle$ is a coherent state on the two torus as developed in Ref. [25]. We have also plotted the complementary Schmidt vectors from tracing out the first degree of freedom and will therefore give the (q_2,p_2) coordinates of any classical structure. The fixed point $(0.5,0,0,0)$ is clearly seen projected onto the two subspaces in the Husimis, thus confirming our earlier statement that the state is “scarred” by this orbit. In general we may expect that periodic orbits scarring the states will be seen in their projections in the Husimis of their principal Schmidt vectors.

The full Husimi distribution is of course 4D and taxes our visualization abilities. The above may be compared to a similar approach that has already been in use when 4D Husimis of 2D eigenfunctions of chaotic oscillators with two degrees of freedom were analyzed via their “quantum surface of sections” [26]. The difference is that the Schmidt states provide a much more complete and systematic way of analyzing higher-dimensional wave functions than the somewhat *ad hoc*, though useful, constructions thus far in use. It has been shown for 2D maps and two degree of freedom flows (which are equivalent) that the zeros of the Husimi distribution, dubbed as “stellar representations,” provide a unique description of the eigenfunctions [27]. The stellar representation of Schmidt vectors may provide a way of avoiding complex functions in two variables; as each vector and its correlated partner will have N zeros each and there are N such pairs, we would have a total of $2N^2$ zeros. Of course these in themselves are not sufficient to specify the state (as we need the eigenvalues of the reduced matrix as well), but we have seen that important information about the states is already present in the Schmidt vectors and must be reflected in their zeros. Calculations not presented here indeed confirm this.

B. Time-dependent properties

We dwell briefly on time-dependent properties. While for wave functions on the full Hilbert space, time-dependent properties may largely be derived from the stationary one, the situation is not entirely obvious when we restrict ourselves to reduced density matrices, or “shadows” in restricted subspaces, if we take an arbitrary (nonstationary) state $|\phi_0\rangle$ and evolve it according to $|\phi(T)\rangle = \mathcal{U}^T|\phi_0\rangle$. The reduced density matrix at any time T cannot be derived based solely on the reduced density matrices of individual states as

$$\begin{aligned} \rho_1(T) = \text{Tr}_2(|\phi(T)\rangle\langle\phi(T)|) &= \sum_k |\langle\psi_k|\phi_0\rangle|^2 \rho_{1k} \\ &+ \sum_{k \neq l} \exp(i(\psi_k - \psi_l)T) \langle\psi_k|\phi_0\rangle\langle\phi_0|\psi_l\rangle \\ &\times \text{Tr}_2(|\psi_k\rangle\langle\psi_l|), \end{aligned} \quad (14)$$

where ψ_k are eigenangles of the corresponding eigenstates. If we assume a nondegenerate spectrum, the reduced density matrix, *averaged over all time*, is the first sum of the above expression and is simply a weighted sum over the reduced density matrices of individual eigenstates.

Thus we expect, based on our previous discussion of diagonally dominant density matrices of eigenstates, that any arbitrary state’s reduced density matrix will rapidly evolve to a predominantly diagonal one. This is of course reminiscent of “decoherence” phenomena [9,28] and indeed as far as each degree of freedom individually is concerned, it is an open system from which phase information can flow out or decohere. However, the state will evolve in such a way that even the diagonal part of the density matrix is significantly altered, i.e., it is not comparable to a situation wherein a pure state is “reduced” to a classical ensemble by a measurement-

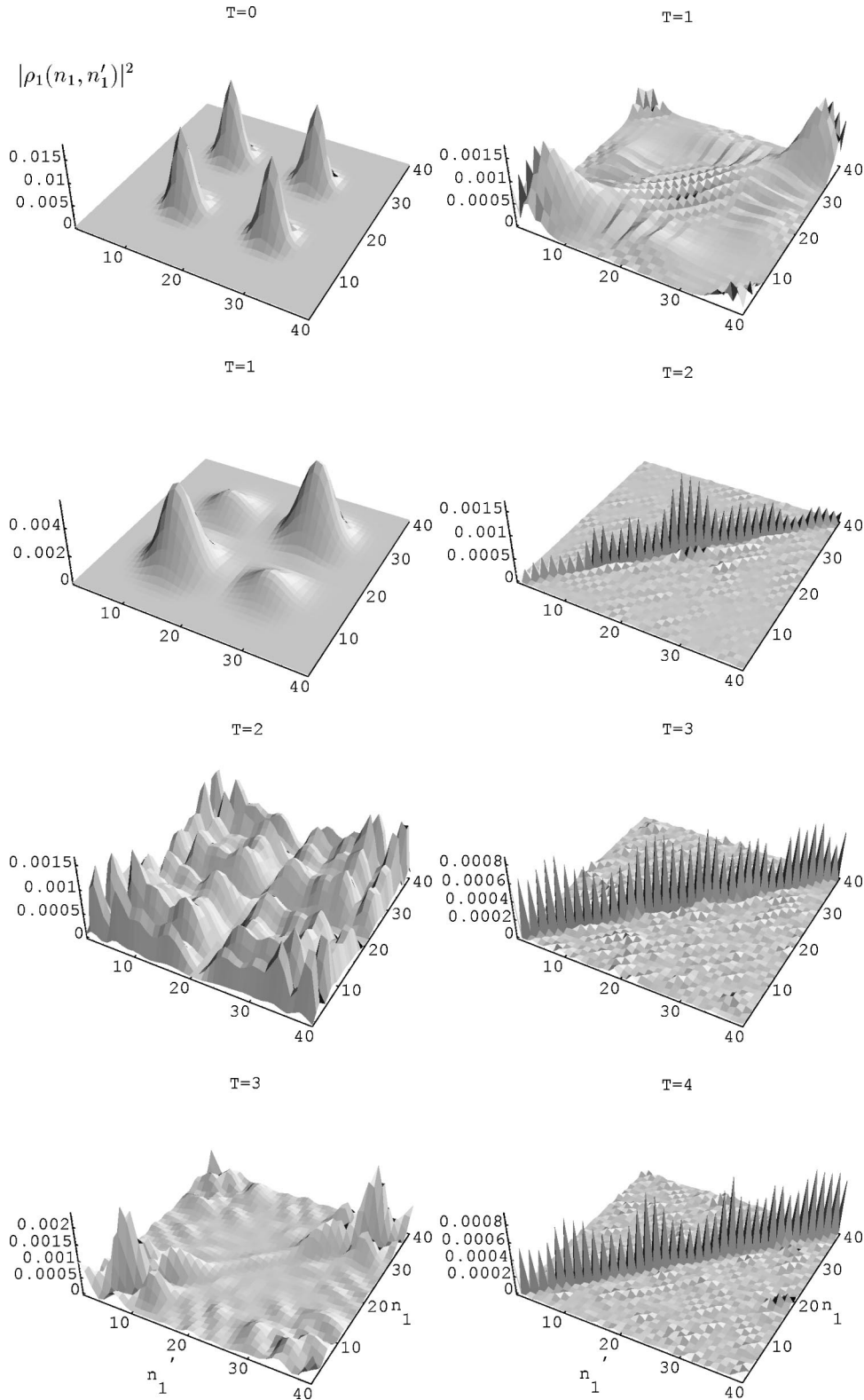


FIG. 9. Time evolution of an initial reduced density matrix shown in the left topmost figure. The left panels correspond to the case $b=0.1$ for evolution over three time steps, while the right corresponds to $b=2$ for evolution over four time steps.

like process. Figure 9 shows the evolution of an initial state, which is the sum of two well-separated Gaussians in position representation. The initial reduced density matrix has large off-diagonal parts. The evolution under a weak coupling produces interesting structures. After even one time step, for low couplings we see that the density matrix has the off-diagonal parts significantly reduced. In fact this picture “looks” like

the one resulting from decoherence [28]. However we are doing a numerically exact computation without using any approximate Master equation. For later times, the case of small coupling or low chaos leads to fairly nondiagonal density matrices, while in comparison the right panel shows the evolution of the same initial state for the first four time units and one sees that effective diagonality is rapidly achieved.

The time-evolving density matrices represent the ‘‘Schmidt paths’’ [20]. If we start with an initially disentangled state, the dynamics when completely chaotic, will quickly rotate the state into those in which there is maximal entanglement in some sense. Is this entanglement different from that observed for stationary states? In fact from numerical calculations not shown here, it seems that these are identical modulo fluctuations. This is unlike the case of the Shannon entropy, which for a time-evolving pure state, is different from a stationary state, basically due to the fact that the time evolving state is in general complex while (for time-reversal symmetric systems as we are currently discussing) the stationary state is real. The typical behavior of the entropy, is as expected, a rise from zero to the constant value of $\ln(0.59N)$ with a rapidity that is a function of the coupling strengths and hence of the chaos in the system.

We briefly also comment on the case when time-reversal invariance is broken. That is achieved in the model studied in this paper by choosing a nonzero β , which is equivalent to an introduction of a magnetic-flux line. While of course much of what has been said already carries over to this case, there may be quantitative differences. For one, the average entanglement of eigenstates is slightly higher at about $\ln(0.61N)$. Thus time-reversal breaking interactions may on the average produce more entanglement, and the reduced density matrices are sensitive to time-reversal breaking.

IV. DISCUSSION

We have presented a variety of essentially numerical results concerning reduced density matrices of chaotic systems. We have studied the entanglement of eigenstates and its possible relationship to localization. Schmidt vectors provide graded information about the nature of localization. We have seen how chaos aids entanglement and it is a small step to extend the universality observed from quantum chaos to reduced density matrices. However, we have not sufficiently explored the density matrices to be able to comment on their randomness or the type of universality we may expect.

There are various ways in which the analysis can be extended. One important direction would be to have more than

two coupled maps, or in general, many particle interacting systems. Such higher-dimensional systems force us to face several problems. One is that Schmidt decomposition is no longer possible, and entanglement becomes much harder to quantify. Ways to measure entanglement in multipartite systems have been proposed recently that may prove to be useful. The other is the increasing complexity of the classical system (if there is one), and the exponentially growing numerical task. Loss of quantum coherence was studied via simple models in Ref. [20] by coupling two state systems to larger Hamiltonians with matrix representations having randomly chosen elements. A natural situation in this context and in the spirit of this paper, is to look at bipartite quantum chaotic systems as we have, but whose dimensionality is unequal.

An important step toward a fundamental understanding of why random matrix modeling must be successful at all was achieved by the use of semiclassical methods and periodic orbit sums [29]. A further direction would be to derive and use semiclassical orbit sums for ‘‘partial traces.’’ This obviously has close links with the Feynman-Vernon path-integral treatment of quantum dissipation. We note that

$$\sum_T \exp(-i\psi T) \text{Tr}_2(\mathcal{U}^T) = \sum_k \sum_m \delta(\psi - \psi_k - 2\pi m) \rho_{1k}, \quad (15)$$

where ψ_k is the eigenangle corresponding to the state whose reduced density matrix is ρ_{1k} . The partial trace of the propagator is therefore naturally a quantity of interest. The classical orbits that will be the stationary paths, will be ‘‘partially periodic’’ orbits, which for a given time T connect two configuration space points in subsystem 1, while appearing periodic in subsystem 2. In general, such semiclassical analysis of partial traces may provide a deeper understanding of various aspects of quantum open systems.

ACKNOWLEDGMENTS

The author thanks Jayendra Bandyopadhyaya for pointing out Ref. [7], and the Indian public for their continued support.

-
- [1] A. Peres, *Quantum Theory: Concepts and Methods* (Kluwer Academic, Dordrecht, 1993).
 - [2] Reviewed by A. Steane, *Rep. Prog. Phys.* **61**, 117 (1998).
 - [3] A. J. Lichtenberg and M. A. Lieberman, *Regular and Chaotic Dynamics* (Springer-Verlag, New York, 1992).
 - [4] M. C. Gutzwiller, *Chaos in Classical and Quantum Mechanics* (Springer-Verlag, New York, 1990); L. E. Reichl, *The Transition to Chaos in Conservative Classical Systems: Quantum Manifestations* (Springer-Verlag, New York, 1992).
 - [5] K. M. O’Connor and W. K. Wootters, e-print quant-ph/0009041.
 - [6] D. Gunlycke, S. Bose, V. M. Kendon, and V. Vedral, e-print quant-ph/0102137.
 - [7] K. Furuya, M. C. Nemes, and G. Q. Pellegrino, *Phys. Rev. Lett.* **80**, 5524 (1998).
 - [8] P. A. Miller and S. Sarkar, *Phys. Rev. E* **60**, 1542 (1999).
 - [9] D. Giulini, E. Joos, C. Kiefer, J. Kupsch, I. -O. Stamatescu, and H. D. Zeh, *Decoherence and the Appearance of a Classical World in Quantum Theory* (Springer-Verlag, Berlin, 1996).
 - [10] A. Bulgac, G. D. Dang, and D. Kusnezov, *Phys. Rev. E* **54**, 3468 (1996).
 - [11] D. Cohen, e-print cond-mat/0103279.
 - [12] J. H. Hannay and M. V. Berry, *Physica D* **1**, 267 (1980).
 - [13] N. L. Balazs and A. Voros, *Ann. Phys. (N.Y.)* **190**, 1 (1989).
 - [14] F. M. Izrailev, *Phys. Rep.* **196**, 299 (1990).
 - [15] R. Schack, *Phys. Rev. A* **57**, 1634 (1998); T. A. Brun and R. Schack, *ibid.* **59**, 2649 (1999).
 - [16] F. L. Moore, J. C. Robinson, C. F. Bharucha, P. E. Williams, and M. G. Raizen, *Phys. Rev. Lett.* **73**, 2974 (1994).
 - [17] C. Froeschlé, *Astrophys. Space Sci.* **14**, 110 (1971); K. Kaneko

- and R. J. Bagley, Phys. Lett. A **110**, 435 (1985); B. Wood, A. J. Lichtenberg, and M. A. Lieberman, Phys. Rev. A **42**, 5885 (1990).
- [18] E. J. Heller, Phys. Rev. Lett. **53**, 1515 (1984); in *Quantum Chaos and Statistical Nuclear Physics*, edited by T. H. Seligman and H. Nishioka (Springer-Verlag, Berlin, 1986).
- [19] S. Popescu and D. Rohrlich, Phys. Rev. A **56**, R3319 (1997).
- [20] A. Albrecht, Phys. Rev. D **46**, 5504 (1992).
- [21] M. S. Santhanam, V. B. Sheorey, and A. Lakshminarayan, Phys. Rev. E **57**, 345 (1998).
- [22] T. A. Brody, J. Flores, J. B. French, P. A. Mello, A. Pandey, and S. S. M. Wong, Rev. Mod. Phys. **53**, 385 (1981).
- [23] L. Kaplan and E. J. Heller, Ann. Phys. (N.Y.) **264**, 171 (1998).
- [24] A. Lakshminarayan, N. R. Cerruti, and S. Tomsovic, Phys. Rev. E **60**, 3992 (1999).
- [25] M. Saraceno, Ann. Phys. (N.Y.) **199**, 37 (1990).
- [26] G. G. de Polavieja, F. Borondo, and R. M. Benito, Int. J. Quantum Chem. **51**, 555 (1994); M .S. Santhanam, Ph.D. thesis, Physical Research Laboratory, Ahmedabad, 1997.
- [27] P. Lebouef and A. Voros, J. Phys. A **23**, 1765 (1990).
- [28] W. H. Zurek, Phys. Today **44**, (Oct.), 36 (1991).
- [29] M. V. Berry, Proc. R. Soc. London, Ser. A **400**, 229 (1985).